Proceedings of the World Congress on Mechanical, Chemical, and Material Engineering (MCM 2015)
Barcelona, Spain – July 20 - 21, 2015
Paper No. 293

Non-Isothermal Displacements with Step-Profile Time Dependent Injections in Homogeneous Porous Media

Qingwang Yuan
Development Research Department, CNOOC Research Institute, China
yuanqw4@cnooc.com.cn

Jalel Azaiez
The University of Calgary, Department of Chemical and Petroleum Engineering
Calgary, Alberta Canada T2N 1N4
azaiez@ucalgary.ca

Abstract -Miscible non-isothermal flow displacements in homogeneous porous media are modeled and analyzed in flows that involve step-profile velocities that alternate between injection and extraction. The viscosity is assumed to vary with both the concentration and the temperature. The flow is governed by the continuity equation, Darcy's law and the convection-diffusion equations for the concentration and temperature with the assumption of thermal equilibrium. The problem is formulated and solved numerically using a combination of the highly accurate spectral-methods based on the Hartley's transform and the finite-difference technique. Non-linear simulations were carried for a variety of parameters to analyse the effects of the time-dependence of the injection velocity on both the solutal and the thermal front. It is found that for the same net flow rate, time-dependent injections affect not only the solutal front but also the thermal from which can become unstable under time-dependent scenarios when it is known to be stable for flows with a constant injection velocity. The results of this study will be used to improve our understanding of the coupling between heat and mass transfer in flows in porous media and to optimize a variety of non-isothermal flow displacements.

Keywords**:** Thermo-Viscous fingering**,** Time-dependent injections, Thermal equilibrium, Homogeneous porous media**,** Numerical simulations.

1. Introduction

Instability at the interface between flowing solutions in a porous medium may takes place as a result of viscosities and/or densities mismatch between the fluids. This instability develops in the form of intruding fingers and is referred to as viscous fingering or Saffman-Taylor instability in case of viscosities mismatch, and as density fingering or Rayleigh-Taylor instability in the case of densities mismatch between the fluids. Extensive reviews of such flows have been presented by Homsy (1987) and McCloud and Maher (1995). These fingering phenomena occur in enhanced oil recovery, fixed bed regeneration, groundwater flows, CO_2 sequestration, and soil remediation and filtration, etc. (Hejazi and Azaiez, 2010). In most cases, viscous fingering is undesirable since it reduces the sweep efficiency, while in others it can be actually desirable as it promotes mixing.

To date, most of the existing studies dealing with this type of instability have been limited to isothermal flows with constant injection velocities. However, in a number of practical applications the displacement velocity is time dependent and involves heat transfer. Examples of such applications include a number of enhanced oil recovery (EOR) processes such as the cyclic steam stimulation (CSS) that involves three stages of injection, soaking and production (Mago et al., 2005) as well as the CO_2 huff-and-puff technique that involves cyclic injection of liquid CO_2 for heavy as well as light oil enhanced recovery (Monger et al., 1991). The success of these processes which can be run as either miscible or immiscible

depends on the importance and duration of each stage of the cycle in conjunction with the efficiency of heat exchange between the different components.

Recently, Dias et al., (2010a; 2010b; 2012) investigated the possibility of attenuating the fingering instability for immiscible flows in a radial geometry using time-dependent flow rates. They reported the optimal flow rates for linear flow regime and nonlinear flow regime. More recently Yuan and Azaiez (2014, a-b) examined the effects of step-size dependent flows on the efficiency and stability of reactive displacements in porous media. The authors showed that it is possible to control the amount of chemical product through a judicious choice of the nature and cycle of the time-dependent displacement. However all the studies examining time-dependent injections have so far been limited to isothermal flows. There are on the other hand a number of studies that have analyzed non-isothermal displacements but under constant injection velocities. These include the studies by Pritchard (2009), Mishra et al. (2010), Islam and Azaiez (2010) and Sajjadi and Azaiez (2013, a-b).

The present study deals with non-isothermal miscible displacements in rectilinear Hele-Shaw cells under sinusoidal flow velocities. The objective of the study is to determine the effects of the frequency, amplitude and phase of the velocity on the hydrodynamic instability and to characterize these effects both qualitatively through concentration contours and quantitatively through the sweep efficiency. The objective is to propose guidelines for the choice of the frequency, amplitude and phase that allow one to control the flow towards either enhancing or attenuating the instability.

2. Flow Configuration and Mathematical Model

A two-dimensional non-isothermal displacement in which both fluids are incompressible, non-reactive and fully miscible is considered. The flow takes place in the horizontal direction in a homogeneous medium of constant porosity ϕ and permeability k.

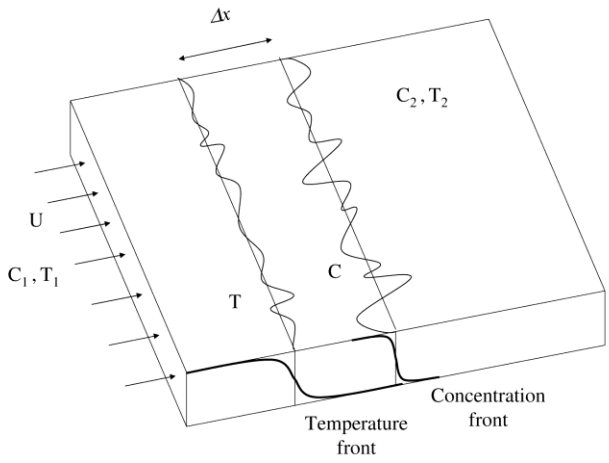

Fig. 1. Schematic of rectilinear Hele-Shaw cell/two-dimensional porous medium.

A fluid (Phase I) of viscosity μ_1 and uniform temperature T_1 is injected with a time-dependent velocity $U(t)$ to displace a second one (Phase II) of viscosity μ_2 and uniform temperature T_2. Here, the direction of the flow is along the x axis and the y axis is parallel to the initial plane of the interface (Figure 1). The length, width and thickness of the medium are denoted by L, W and e respectively. The mathematical model describing the non-isothermal miscible displacement flow involves the conservation of mass and momentum and mass-energy balance equations:

$$\nabla.\mathbf{v} = 0 \tag{1}$$

$$\nabla p = -\frac{\mu}{K}\mathbf{v} \tag{2}$$

$$\frac{\partial C}{\partial t} + \frac{\mathbf{v}}{\phi}.\nabla C = D_C \nabla^2 C \tag{3}$$

$$\frac{\partial T}{\partial t} + \frac{\lambda \mathbf{v}}{\phi}.\nabla T = D_T \nabla^2 T \tag{4}$$

In the above equations, **v**=(*u*,*v*) while ∇ and ∇^2 stand for the gradient and Laplacian operators in the (x,y) plane. Furthermore, *p* represents the pressure, μ the viscosity, *k* the medium permeability and ϕ its porosity. The concentration of the solvent (displacing fluid) is denoted by *C* while the temperature of the solid-fluid system which is assumed to be in local thermal equilibrium is *T*. The corresponding mass and thermal diffusion coefficients are referred to by D_C and D_T, respectively. The above equations model the propagation of two fronts, one associated with temperature and will be referred to as the thermal front while the other corresponds to mass transport and will be called the solutal front. The parameter λ that we shall refer to as the *thermal lag* coefficient can be interpreted as the ratio of the speed of the thermal front to that of the solutal front (Bejan and Nield, 2006, Pritchard, 2009, Islam and Azaiez 2010):

$$\lambda = \frac{\phi \rho_f Cp_f}{\phi \rho_f Cp_f + (1-\phi)\rho_s Cp_s} \tag{5}$$

In the above equation, ρ_s, Cp_s, ρ_f, and Cp_f are the density and heat capacities of the solid phase and the fluid phase respectively. Note that $\lambda \leq 1$ with higher values corresponding to smaller difference between the velocities of concentration and temperature fronts and lower values corresponding to higher rates of dissipation of heat. Throughout this study we will assume that the changes in the fluid density and heat capacity are sufficiently small such that λ can be considered constant.

The governing equations are made dimensionless as in Islam and Azaiez (2005) and Yuan and Azaiez 2014, and are expressed in a Lagrangian reference frame moving with the dimensionless displacement velocity $u_f(t)$. This results in the following dimensionless equations (using the same notation as for dimensional quantities):

$$\nabla.\mathbf{v} = 0 \tag{6}$$

$$\nabla \mathrm{p} = -\mu[\mathbf{v} + \mathrm{u_f}(\mathrm{t})\mathbf{i}] \tag{7}$$

$$\frac{\partial C}{\partial t} + \mathbf{v}.\nabla \mathrm{C} = \nabla^2 \mathrm{C} \tag{8}$$

$$\frac{\partial \theta}{\partial t} + \lambda \mathbf{v}.\nabla \theta + (\lambda - 1)\frac{\partial \theta}{\partial \mathrm{x}} = Le \nabla^2 \theta \tag{9}$$

In the above equations $Le = D_T/D_C = Pe_C/Pe_T$ is the Lewis number where Pe_C and Pe_T are the solutal and thermal Péclet numbers, respectively. Two additional dimensionless groups are also involved, namely the Péclet number $Pe = UL/D_C$ and the cell aspect-ratio $A = L/H$ that appear in the boundary conditions (Sajjadi and Azaiez 2013). To complete the model, a form for the dependence of the viscosity on concentration and temperature must be specified. Following Pritchard (2009), Islam and Azaiez (2010) and Sajjadi and Azaiez (2013), exponential dependence is adopted:

$$\mu(C,\theta) = \exp[\beta_C(1-c) + \beta_T(1-\theta)] \tag{10}$$

In this equation β_c is the natural logarithm of the viscosity ratio μ_1/μ_2 in an isothermal miscible displacement and β_T is the natural logarithm of the ratio of the viscosity μ_{1T}/μ_{2T} in a single fluid flow with two different temperatures at the inlet and outlet boundaries.

3. Numerical Procedure

The equations are expressed using a stream-function vorticity formulation, where the velocity field, the stream-function ψ and the vorticity w (Hejazi and Azaiez 2013, Yuan and Azaiez 2014, a-b). With this formulation, the continuity equation is satisfied automatically and the governing equations take the forms:

$$\frac{\partial C}{\partial t} + \frac{\partial \psi}{\partial y}\frac{\partial C}{\partial x} - \frac{\partial \psi}{\partial x}\frac{\partial C}{\partial y} = \frac{\partial^2 C}{\partial x^2} + \frac{\partial^2 C}{\partial y^2} \tag{11}$$

$$\frac{\partial \theta}{\partial t} + \lambda\left(\frac{\partial \psi}{\partial y}\frac{\partial \theta}{\partial x} - \frac{\partial \psi}{\partial x}\frac{\partial \theta}{\partial y}\right) + (\lambda - 1)\frac{\partial \theta}{\partial x} = Le\left(\frac{\partial^2 \theta}{\partial x^2} + \frac{\partial^2 \theta}{\partial y^2}\right) \tag{12}$$

$$w = \beta_C\left[\frac{\partial \psi}{\partial x}\frac{\partial C}{\partial x} + \left(\frac{\partial \psi}{\partial y} + u_f(t)\right)\frac{\partial C}{\partial y}\right] + \beta_T\left[\frac{\partial \psi}{\partial x}\frac{\partial \theta}{\partial x} + \left(\frac{\partial \psi}{\partial y} + u_f(t)\right)\frac{\partial \theta}{\partial y}\right] \tag{13}$$

$$\nabla^2 \psi = -w \tag{14}$$

The partial differential and algebraic equations are solved using a highly accurate pseudo-spectral method based on the Hartley transform in conjunction with a semi-implicit predictor-corrector time-stepping method along with an operator-splitting algorithm (Islam and Azaiez 2005).

The code was validated by comparing the concentration contours for constant velocity under isothermal with the study by Islam and Azaiez (2005) and for non-isothermal displacements with the results of Islam and Azaiez (2010) and Sajjadi and Azaiez (2013b). Furthermore, the convergence of the numerical solution was examined by considering cases with different spatial resolutions varying from 128x128 to 512x512 while varying the time step accordingly. Since a resolution of 256x256 resulted in finger structures similar to those obtained with larger number of grid points, it was adopted in all subsequent simulations.

4. Results

In this section, the flow dynamics will be analyzed in the case of are solved numerically in the case of step-size time dependent injection velocity profiles $u_f(t)$ with a period T. Such types of velocity profiles correspond to many practical applications where the displacing fluid is injected and produced (or soaked) at constant velocities in a certain period of time, or vice versa. Each cycle consists of two stages. The first with a constant velocity ($u_f(t) = u_1$) lasts a time (t_1) and is followed by the second stage where the velocity switches to a new value ($u_f(t) = u_2$) and lasts a time ($t_2 = T - t_1$). The objective is to compare the results with those of a constant injection velocity ($u = 1$), which requires the average velocity over a period to be also equal to one ($\overline{u_f(t)} = 1$). This implies that the net injected flow in both the time-dependent and constant velocity displacements is the same. This requires that $t_1 = (\overline{u_f(t)} - u_2)T/(u_1 - u_2) = (1 - u_2)T/(u_1 - u_2)$.

Hence, the time-dependent displacement is fully characterized by both u_1, u_2 and the cycle period T. It should be also mentioned that in cases where the displacement velocity changes sign and the process switches from injection (positive velocity) to extraction (negative velocity) or vice versa, zones with

positive mobility ratios will change from unstable to stable state, or vice versa. This is also true for zones with negative mobility ratios. However for consistency, the zones will be referred to as stable or unstable based on the flow displacement of the constant injection velocity.

In all that follows, the following parameters are fixed as A=2 and Pe=500, Le=1, and λ =0.75. For brevity and illustration purposes, the time sequences will not be always presented necessarily at the same time intervals, and only the frames that reveal new and interesting finger structures that help in the discussion, are shown. In all contours, the red and blue colour fields correspond to the displacing and displaced fluid, respectively.

4. 1. Non-Isothermal Flows with Constant Injection Velocity

In this section, different scenarios of non-isothermal displacements with unit injection velocity are presented. Figure 2 shows the concentration contours for four different scenarios that correspond to positive or negative values of the mobility ratios. In the case of a flow where a viscous cold fluid displaces a less viscous hot one ($\beta_c = -3, \beta_T = -3$), the interface is stable. This is expected since in this case both the solutal and thermal fronts are under favourable displacement conditions. The interface diffuses with time but no fingers develop (Fig2-a). When the thermal front is unstable while the solutal lone is stable ($\beta_c = -3, \beta_T = 3$), instabilities grow on the thermal front and due to the coupling, this results in rather diffuse instabilities that are observed in the concentration contours of Fig2-b at late times. As discussed by Islam and Azaiez (2010) and Sajjadi and Azaiez (2013b), this coupling is stronger for larger values of the lag coefficient λ .

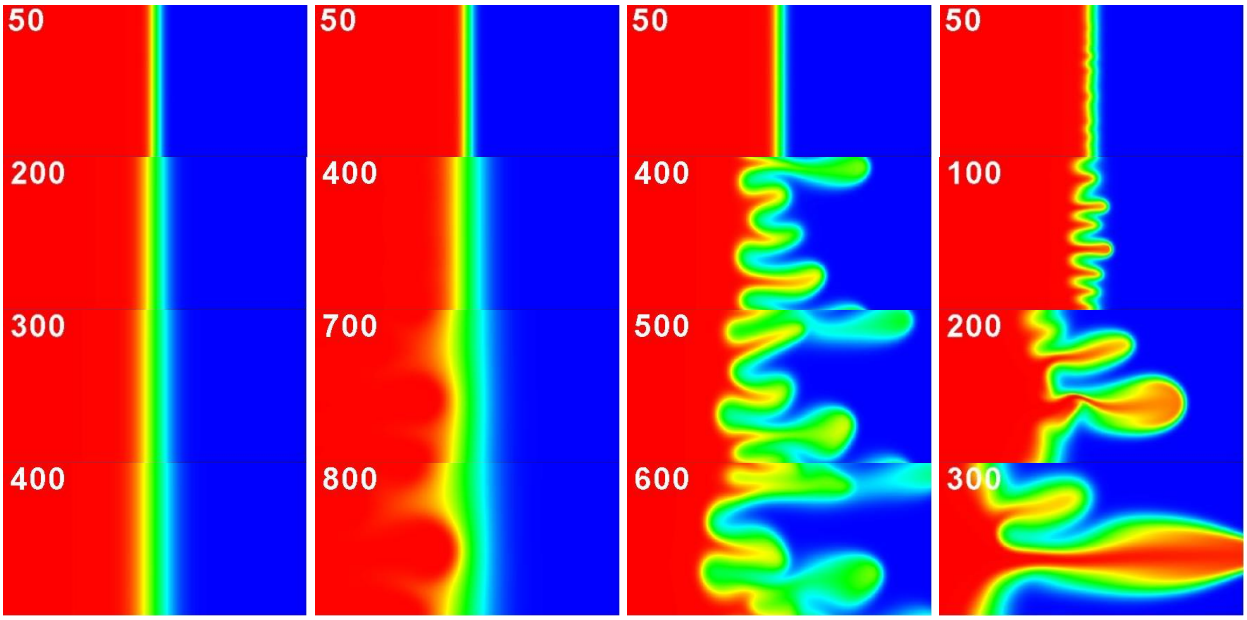

(a) (b) (c) (d)

Fig. 2. Concentration profiles for constant injection velocity at different times for (a) $\beta_c = -3, \beta_T = -3$, (b) $\beta_c = -3, \beta_T = 3$, (c) $\beta_c = 3, \beta_T = -3$, (d) $\beta_c = 3, \beta_T = 3$.

Figure2-c and Figure2-d depict the results where the solutal viscosity is unfavourable ($\beta_c = 3 > 0$) and the thermal one is either favourable ($\beta_T = -3$) or unfavourable ($\beta_T = 3$), respectively. In these cases, fingers develop rapidly resulting in a rapid breakthrough, notably in the case where both the solutal and thermal fronts are unstable (Fig2-d). It must also be noted that the number of fingers are larger and their structures are more complex in this last case.

4. 2. Non-Isothermal Flows with Time-Dependent Injection Velocity

The development of the flow is now analysed in the case of a step-size time-dependent flow displacement. The analysis will focus on a scenario where the displacement is initiated by an injection followed by extraction ($u_1 = 3, u_2 = -1$). It will also be limited to the case of a less viscous cold fluid displacing a more viscous one ($\beta_c = 3, \beta_T = -3$). As discussed in the previous section, the flow leads to an unstable solutal front but the growth of the fingers is mitigated by the stable thermal front. Fig.3 show the concentration contours for a constant injection velocity ($u = 1$), and two time-dependent flows ($u_1 = 3, u_2 = -1$) with a period $T = 200$ (case1) and $T = 400$ (case2).

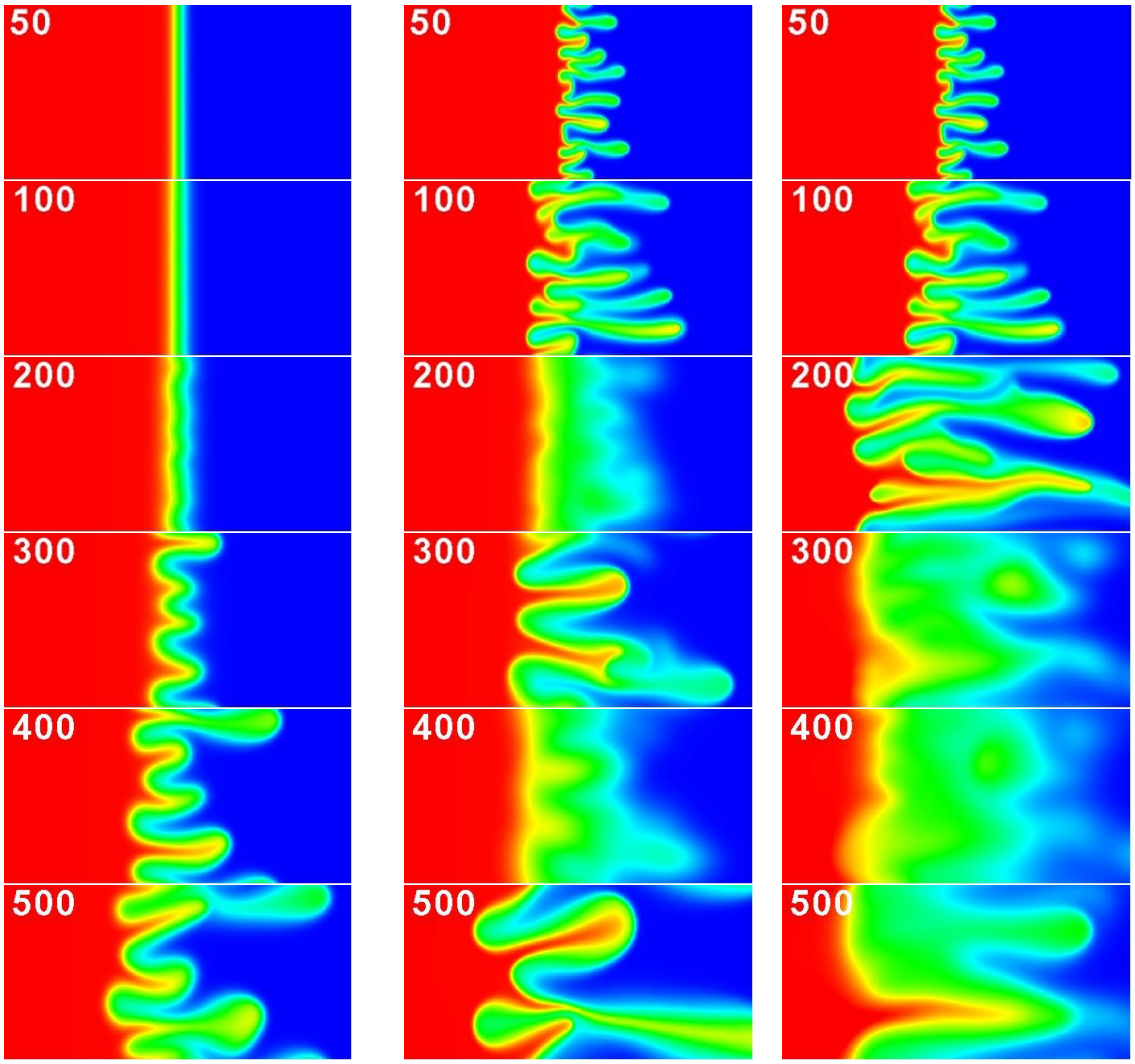

(a) (b) (c)

Fig. 3. Concentration profiles for constant and time-dependent injection velocities at different times and for different periods. $\beta_c = 3, \beta_T = -3, u_1 = 3, u_2 = -1$. (a) Constant velocity, (b) $T = 200$, (c) $T = 400$.

It is clear that in the early stages of the displacement, the time-dependent flows are more unstable than their constant injection velocity counterpart. Fingers are well developed by t=50 while none have developed in the case of the constant unit velocity. Moreover, up to a time corresponding to half a period of case1, the structures are identical for both time-dependent injection flows. This is not surprising since up to that time the velocity is the same for both cases. Past this time, the flow in case1 moves to an extraction mode where the flow reverses and as a consequence the displacement becomes favourable. This flow reversal is responsible for an attenuation of the instability and the interface becomes diffuse with no

sharp fingers. At the same time, case2 is still in the injection mode and the fingers are able to develop and extend further in the flow. The situation is reversed past the half-period of case2, where the flow now shifts to extraction and the fingers are strongly damped in case2 while they are reinvigorated in case1. Actually, as the long stage of extraction, case2 ends up with a very wide diffused interface that subsequently is not propitious for the growth of strong fingers. In this flow scenario, case1 ends up being the most unstable displacement and results in the earliest breakthrough time, while case2 is the least unstable one and exhibits an interface that is less unstable than that of the constant injection flow.

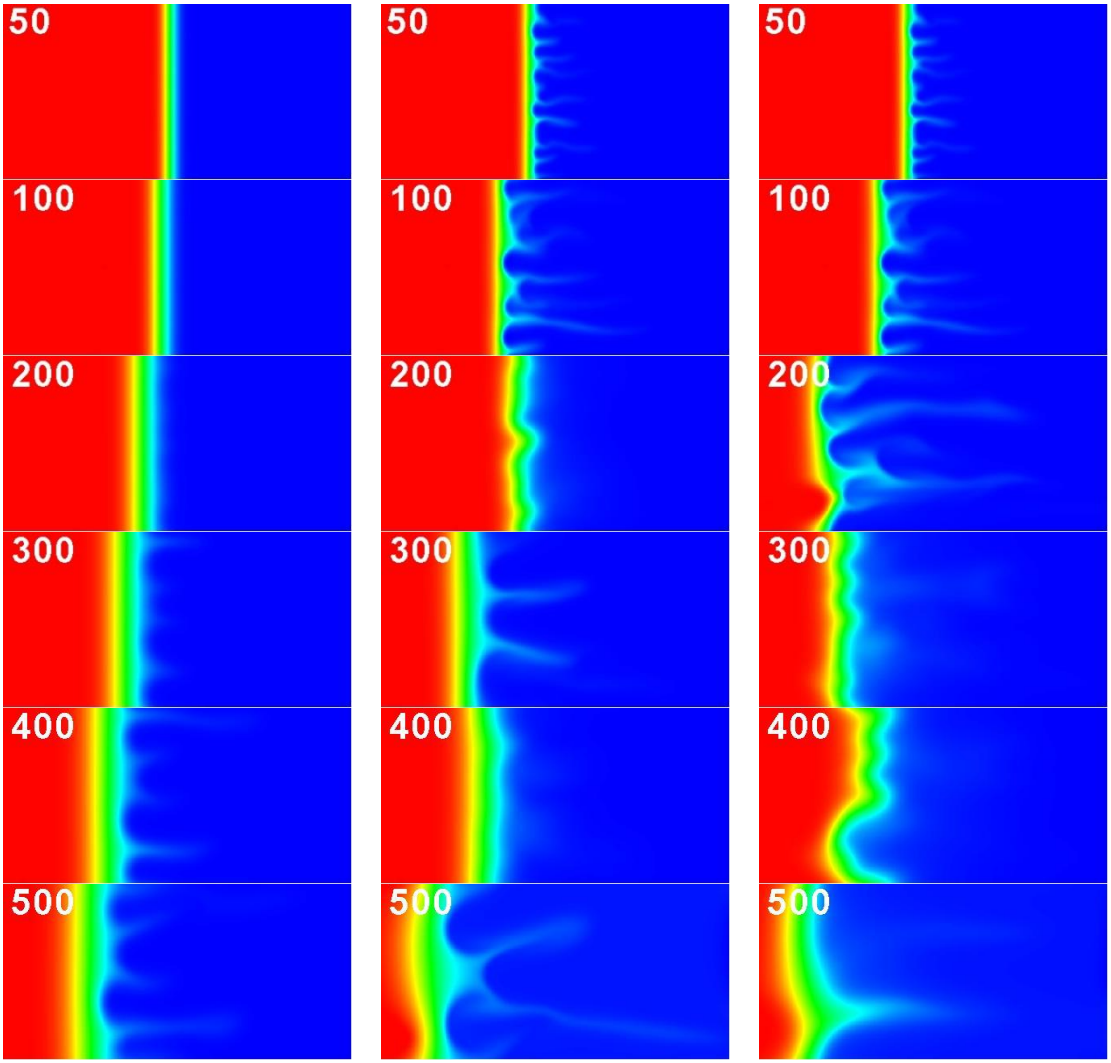

(a) (b) (c)

Fig. 4. Temperature profiles for constant and time-dependent injection velocities at different times and for different periods. $\beta_c = 3, \beta_T = -3, u_1 = 3, u_2 = -1$. (a) Constant velocity, (b) $T = 200$, (c) $T = 400$.

The effects of the time-dependent flow on the corresponding thermal front are depicted in Figure 4. It is clear that in the constant injection flow, the thermal front is basically stable and the small wavy interface is attributed to the coupling with the solutal front. This coupling is however short and the fronts separate as the thermal front recedes due to heat losses to the porous medium while the solutal front advances with strong fingers. This changes when the injection velocity is time-dependent and the coupling is now stronger and more lasting leading to shaper and more developed thermos-fingers. This is due to two factors. The first one is a natural result of the more unstable solutal front that is able to grow at the early stages of the displacement when the two fronts are still close. This allows the thermal front to

develop instabilities (see Fig.4b-c at t=50 and t=100) when that of the constant injection is still stable. Even though these thermos-fingers are not well developed they become the precursors of the fingers that develop later even when the flow reverses into an extraction. The second factor is associated with the initial stronger injection velocity ($u_1 = 3$) that delays the effects of heat diffusion into the porous medium and help maintain a sharper thermal front where fingers can grow easier. It is interesting that in spite of the flow reversal, the thermos fingers were able to maintain their growth and were not supressed even at late times.

5. Conclusion

In this study, the effects of time-dependent step-profile injection velocities on the development of fingering instabilities in homogeneous porous media were examined. The analysis focuses on non-isothermal miscible displacements where both heat and mas are transported by the flow. The development and progress of the instabilities are illustrated through iso-surfaces of both the concentration and the temperature of the fluids. The dynamics of the flow were analysed for an injection-extraction process and compared with those arising from a constant injection velocity that results in the same average flow rate. It is found that the time-dependent velocity affects the hydrodynamic instability and in particular it has an important impact on the thermal front due to the coupling between the solutal and the thermal fronts. The results of the study will be a cornerstone for understanding and optimizing processes that involve time-dependent injections of hot/cold fluids in porous media.

Acknowledgements

Financial support from the China Scholarship Council (CSC) and the Natural Sciences and Engineering Research Council of Canada (NSERC) are gratefully acknowledged. The authors would like also to acknowledge WestGrid for providing computational resources.

References

Bejan, A., & Nield, D. (2006). Convection in Porous Media, 3rd Edition. Springer.

Dias, E. O., Parisio, F., & Miranda, J. A. (2010a). Suppression Of Viscous Fluid Fingering: A Piecewise-Constant Injection Process. *Phys. Rev. E.*, 82, 067301-1–067301-4.

Dias, E. O., & Miranda, J. A. (2010b). Control Of Radial Fingering Patterns: A Weakly Nonlinear Approach. *Phys. Rev. E.*, 81, 016312-1–016312-7.

Dias, E. O., Alvarez-Lacalle, E., & Carvalho, M. S. (2012). Minimization Of Viscous Fluid Fingering: A Variational Scheme For Optimal Flow Rates. *Phys. Rev. Lett.*, 109, 144502-1–144502-5.

Hejazi, H., & Azaiez, J. (2013). Nonlinear Simulation Of Transverse Flow Interactions With Chemically Driven Convective Mixing In Porous Media. *Water Res. Res.*, 49, 8, 4607-4618.

Homsy, G.M. (1987). Viscous Fingering In Porous Media. *Ann. Rev. Fluid Mech.*, 19, 271-311.

Islam, N., & Azaiez, J. (2005). Fully Implicit Finite Difference-Pseudo Spectral Method For The Simulation Of High Mobility-Ratio Miscible Displacements. *Int. J. Num. Meth. Fluid.*, 47, 161-183.

Islam, N., & Azaiez, J. (2010). Miscible Thermo-Viscous Fingering Instability In Porous Media: Part 2: Numerical Simulations. *Transp. Porous Media*, 84**,** 845-861**.**

Mago, A., Barrufet, M., & Nogueira, M. (2005). Assessing The Impact Of Oil Viscosity Mixing Rules In Cyclic Steam Stimulation Of Extra-Heavy Oils. *Proc.. of the SPE Annual Technical Conference and Exhibition*, SPE 95643-1-7.

McCloud, K.V., & Maher, J.V. (1995). Experimental Perturbations to Saffman-Taylor Flow. *Physics Reports*, 260, 139-185.

Mishra, M., Trevelyan, P. M., Almarcha, C., & De Wit, A. (2010). Influence Of Double Diffusive Effects On Miscible Viscous Fingering. *Physical Review Letters*, 105, 204501-204504.

Monger, T., Ramos, J., & Thomas, J. (1991). Light Oil Recovery From Cyclic CO2 Injection: Influence Of Low Pressures Impure CO2, And Reservoir Gas. *SPE J.*, 6, 25-32.

Pritchard, D. (2009). The Linear Stability Of Double-Diffusive Miscible Rectilinear Displacements In A Hele-Shaw Cell. *Eur. J. of Mechanics, B/Fluids*, 28, 564-577.

Sajjadi, M., & Azaiez, J. (2013a). Scaling And Unified Characterization Of Flow Instabilities In Layered Heterogeneous Porous Media. *Phys. Rev. E.,* 88**,** 033017-1–033017-12.

Sajjadi, M., & Azaiez, J. (2013b). Dynamics Of Fluid Flow And Heat Transfer In Homogeneous Porous Media. *Can. J. Chem. Eng.,* 91**,** 687-697.

Yuan, Q., & Azaiez, J. (2014a). Cyclic Time-Dependent Reactive Flow Displacements In Porous Media. *Chem. Eng. Sci.*, 109, 136-146.

Yuan, Q., & Azaiez, J. (2014b). Miscible Displacements In Porous Media With Time-Dependent Injection Velocities. *Transp. Porous Media*, 104, 57-76.